Inorganic Chemistry

ARTICLE

pubs.acs.org/IC

Unprecedented 1,3-Diaza[3]ferrocenophane Scaffold as Molecular Probe for Anions†

Antonia Sola,[‡] Raúl A. Orenes,[§] María Ángeles García,[∥] Rosa M. Claramunt,[∥] Ibon Alkorta,[⊥] José Elguero,[⊥] Alberto Tárraga,[*,‡] and Pedro Molina[*,‡]

[‡]Departamento de Química Orgánica, Facultad de Química, and [§]Servicio de Apoyo a la Investigación (SAI), Campus de Espinardo, Universidad de Murcia, E-30100 Murcia, Spain

[∥]Departamento de Química Orgánica y Bio-Orgánica, Facultad de Ciencias, UNED, Senda del Rey 9, E-28040 Madrid, Spain, and [⊥]Instituto de Química Médica (CSIC), Juan de la Cierva, 3, E-28006 Madrid, Spain

Supporting Information

ABSTRACT: The guanidine unit in the guise of 2-aminoimidazole in the new structural motif 2-arylamino-1,3-diaza-[3]ferrocenophane **4** acts as a binding site for anions. The electrochemical behavior of this compound has been studied by cyclic voltammetry (CV) and differential pulse voltammetry (DPV) and was found to exhibit a quasi reversible oxidation peak, associated to the Fe(II)/Fe(III) redox couple (Ep = 440 mV), and a non-reversible oxidation wave (Ep = 817 mV), probably associated to the oxidation of the C═N unit present in the guanidine bridge. Recognition of AcO^-, $PhCO_2^-$, F^-, Cl^-, and Br^- anions by the free receptor and the less basic anions Br^-, Cl^-, and NO_3^- by its monoprotonated form takes place by unusual redox-ratiometric measurements and spectroscopic (^{1}H NMR and UV−vis) changes.

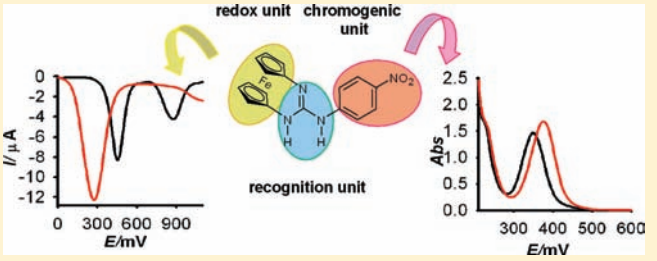

INTRODUCTION

The recognition and sensing of anions has emerged recently as a key research area within the generalized field of supramolecular chemistry for the important role placed by anions in biological, industrial, and environmental processes.[1] In particular, designing receptors capable of anion binding by hydrogen bonding continues to be an area of active research.[2] The guanidine function, because of its amphoteric nature, has a rich history in biological,[3] and bioinspired molecular recognition.[4] The guanidinium group within a variety of molecular architectures forms strong noncovalent interactions with anionic groups through hydrogen-bonding and charge-pairing interactions. In addition, deprotonated guanidines (guanidinates) have the potential to develop into valuable ancillary ligands in coordination and organometallic chemistry,[5] although the straightforward coordination of neutral guanidines to metal centers remains comparatively underdeveloped,[6] and metal-guanidinyl complexes are barely known and unexplored.[7]

Ferrocene has largely proved to be a simple and remarkably robust building block for the preparation of derivatives which have been considered as prototype chemosensor molecules displaying interesting electrochemical-sensing properties. In ferrocene-based ligands, cation binding at an adjacent receptor site induces a positive shift in the redox potential of the ferrocene-ferrocenium couple by through-space electrostatic communication, and the complexing ability of the ligand can be switched on and off by varying the applied electrochemical potential.[8] Recently, some papers have reported functionalized ferrocene derivatives bearing chromogenic or fluorogenic moieties, which display multichannel signaling for anions.[9] Despite the rich chemistry of guanidines, as the binding site, and ferrocene, as the redox signaling unit, only two examples of guanidinyl-ferrocene ligands have been described.[10] In this work, we combine in a highly preorganized system the redox activity of the ferrocene group with the chromogenic behavior of the *p*-nitrophenyl ring and the binding ability of the guanidine group.

In the benzimidazole-like receptor **4**, 2-arylamino-1,3-diaza-[3]ferrocenophane, the redox reporter (ferrocene) is integrated within the ferrocenophanic unit while the chromogenic fragment (*p*-nitrophenyl ring) is linked to the guest guanidine (in the guise of 2-aminoimidazole) anion binding site, which is embedded into the framework of the "ferrimidazole" system. Despite its simple nature, this system may be altered following receptor-anion interaction thus providing redox, colorimetric, and spectral sensing of the recognition event.

EXPERIMENTAL SECTION

General Comments. Melting point was determined on a hot-plate melting point apparatus and are uncorrected. Routine ^{1}H- and ^{13}C NMR spectra were recorded at 200 and 50 MHz, respectively. Chemical shifts

Received: November 19, 2010
Published: February 14, 2011

refer to signals of tetramethylsilane (TMS) in the case of ^{1}H and ^{13}C spectra. The external standard used in the NMR titrations was also TMS. The following abbreviations are used to represent the multiplicity of the signals: st (pseudotriplet), d (doublet), and q (quaternary carbon atom).

UV−vis spectra were carried out in a UV−vis−NIR spectrophotometer using a dissolution cell of 10 mm path. The samples were solved in CH_3CN ($c = 1 \times 10^{-4}$ M), and the spectra were recorded with the spectra background corrected before and after of the sequential additions of aliquots of 0.5 equiv of anions in CH_3CN ($c = 2.5 \times 10^{-2}$ M).

Cyclic voltammetry (CV) and differential pulse voltammetry (DPV) techniques were performed with a conventional three-electrode configuration consisting of platinum working and auxiliary electrodes and a SCE reference electrode. The experiments were carried out with a 10^{-3} M solution of sample in CH_3CN containing 0.1 M $[(n\text{-}C_4H_9)_4N]PF_6$ ($TBAPF_6$) as supporting electrolyte. All the potential values reported are relative to the decamethylferrocene (DMFc) couple at room temperature. Deoxygenation of the solutions was achieved by bubbling nitrogen for at least 10 min, and the working electrode was cleaned after each run. The cyclic voltammograms were recorded with a scan rate increasing from 0.05 to 1.00 V s^{-1}, while the DPV were recorded at a scan rate of 100 mV s^{-1} with a pulse high of 10 mV and a step time of 50 ms. Typically, receptor (1×10^{-3} M) was dissolved in CH_3CN (5 mL) and $TBAPF_6$ (base electrolyte) (0.170 g) added. The guest under investigation was then added as a 0.1 M solution in appropriate solvent using a microsyringe while the cyclic voltammetric properties of the solution were monitored. Decamethylferrocene (DMFc) was used as an external reference both for potential calibration and for reversibility criteria. Under similar conditions the DMFc has $E_{1/2} = -0.07$ V versus SCE and $E_{1/2} = -0.46$ V versus ferrocene, and the anodic peak-cathodic peak separation is 67 mV.

Suitable single crystals of **1** for X-ray structural analysis were obtained by slow evaporation of a solution of the solid in acetone. The diffraction data were collected with a Bruker Smart APEX diffractometer using a monochromated Mo Kα radiation ($\lambda = 0.71073$ Å) in ω-scan mode. The structure was solved by direct methods, and all non-hydrogen atoms refined anisotropically on F^2 using the program SHELXL-97. All H atoms were initially located in a difference Fourier map and refined using a riding model, except for the NH hydrogens, which were refined freely. The ordered methyl groups of the acetone were refined by using rigid groups.

Solid state ^{13}C (100.73 MHz) and ^{15}N (40.60 MHz) CPMAS NMR spectra were obtained on a Bruker WB 400 spectrometer at 298 K using a 4 mm DVT probehead. Samples were carefully packed in 4-mm diameter cylindrical zirconia rotors with Kel-F end-caps. Operating conditions involved 3.2 μs 90° ^{1}H pulses and decoupling field strength of 78.1 kHz by TPPM sequence. The NQS (Non Quaternary Suppression) technique to observe only the quaternary C-atoms was employed. ^{13}C spectra were originally referenced to a glycine sample and then the chemical shifts were recalculated to the Me_4Si [for the carbonyl atom δ (glycine) = 176.1 ppm] and ^{15}N spectra to $^{15}NH_4Cl$ and then converted to nitromethane scale using the relationship: $\delta^{15}N$ (nitromethane) = $\delta^{15}N$(ammonium chloride) − 338.1 ppm. The typical acquisition parameters for ^{13}C CPMAS were as follows: spectral width, 40 kHz; recycle delay, 5 s; acquisition time, 30 ms; contact time, 2 ms; and spin rate, 12 kHz. And for ^{15}N CPMAS they were as follows: spectral width, 40 kHz; recycle delay, 5 s; acquisition time, 35 ms; contact time, 7 ms; and spin rate, 6 kHz.

Solution NMR spectra were recorded on a Bruker DRX 400 (9.4 T, 400.13 MHz for ^{1}H) spectrometer with a 5-mm QNP-probe equipped with a z-gradient coil, at 298 K. Chemical shifts (δ in ppm) are given from internal solvent, $CDCl_3$ 7.26 for ^{1}H. Typical parameters for ^{1}H NMR spectra were spectral width 4800 Hz and pulse width 9.25 μs at an attenuation level of −3 dB.

Computational Details. All the molecules were optimized at the B3LYP/6-31G(d) level[11] where frequencies[12] were calculated to verify that all of them were minima (number of imaginary frequencies = 0). These optimized geometries were further optimized at the B3LYP/6-311++G(d,p) level.[13] Absolute shieldings and NICS(1)[14] were calculated within the GIAO approximation[15] on the last optimized geometries [GIAO/B3LYP/6-311++G(d,p)]. These calculations were carried using the facilities of the Gaussian 03 software.[16] The electron density of the systems has been analyzed with the Atoms in Molecules (AIM) methodology[17] and the MORPHY program.[18] The absolute shieldings were transformed into chemical shifts (δ, ppm) using three empirical equations we have established previously:[19]

$$\delta^{13}C = 175.7 - 0.963\sigma^{13}C$$

$$\delta^{15}N = -152.0 - 0.946\sigma^{15}N$$

$$\delta^{1}H = 31.0 - 0.97\sigma^{1}H$$

Preparation of 2-(4-Nitrophenyl)amino-1,3-diazaferrocenophane 4. To a solution of *p*-nitrophenylisocyanate in dry CH_2Cl_2 (40 mL) a solution of 1,1′-bis(triphenylphosphoranylidenamino) ferrocene **1** (0.2 g, 0.27 mmol) in the same solvent (10 mL) was added dropwise, and the solution was stirred for 1 h at room temperature. The solvent was removed under vacuum, and the resulting residue was chromatographed on a silica-gel column using ethyl acetate/*n*-hexane (6/4) as eluent to give **4** which was crystallized from CH_2Cl_2/Et_2O (1:2). Yield: 74 mg (75%); mp 174−176 °C (d). ^{1}H NMR (200 MHz, acetone-d_6): δ 3.84 (st, 2H), 4.09 (st, 2H), 7.91 (d, 1H, $J = 9.4$ Hz), 8.16 (d, 2H, $J = 9.4$ Hz). ^{13}C NMR (50 MHz, acetone-d_6): δ 67.7 (2×CH), 69.4 (2×CH), 118.3 (CH), 125.2 (CH), 141.6 (q), 148.9 (q), 153.0 (q). EIMS, *m*/*z* (relative intensity): 362 (M^+, 100), 316 (42), 224 (55). Anal. Calcd for $C_{17}H_{14}FeN_4O_2$: C, 56.38; H, 3.90; N, 15.47. Found: C, 56.63; H, 3.68; N, 15.58.

RESULTS AND DISCUSSION

Synthesis, Structure, and Tautomeric Studies. The aza-Wittig protocol[20] was the method of choice for building up the 2-aminoimidazole architecture in **4**, so that the bis(iminophosphorane) **1**, readily available from 1,1′-diazidoferrocene and triphenylphosphine[21] was used as starting material. Receptor **4** was obtained in 75% yield from the aza-Wittig reaction between the bis(iminophosphorane) **1** and *p*-nitrophenylisocyanate in dry dichloromethane at room temperature. Formation of compound **4** can be explained by an initial aza-Wittig-type reaction between one iminophosphorane group of compound **1** and 1 equiv of the isocyanate to give the carbodiimide **2**, which undergoes cyclization by nucleophilic attack of the nitrogen atom of the remaining iminophosphorane moiety on the central carbon atom of the carbodiimide functionality to give the zwitterionic compound **3**. This compound undergoes hydrolytic cleavage during the workup to give **4** (Scheme 1). This mechanism is in accordance with previous results obtained from the aza-Wittig reaction of aryl, vinyl bis(iminophosphoranes) with aryl isocyanates substituted with an electron-withdrawing group.[22]

Crystals suitable for X-ray diffraction analysis were obtained which unambiguously demonstrate the proposed structure for compound **4**. A summary of crystallographic data collection parameters and refinement parameters for **4** are compiled in the Supporting Information (see Table 1 in Supporting Information). Compound **4** crystallizes in the orthorhombic space group *Pbca*. Figure 1 shows the ORTEP drawing of the molecule structure of **4** with the atomic numbering scheme. In the ferrocenyl moiety, the two cyclopentadienyl (Cp) rings are

Scheme 1. Synthesis of the Ferrocene-Imidazole 4[a]

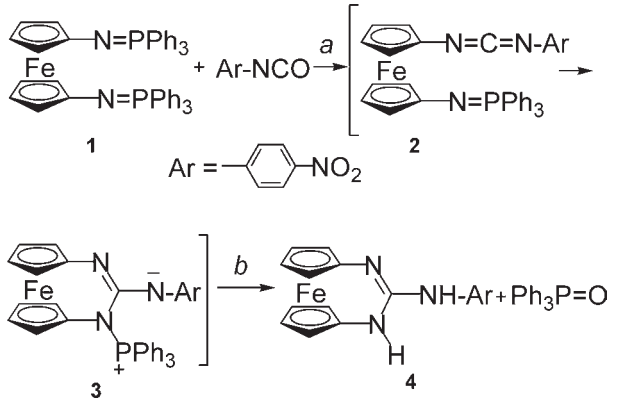

[a] **Conditions**: (a) Dry CH_2Cl_2, r.t. 1 h; (b) work up.

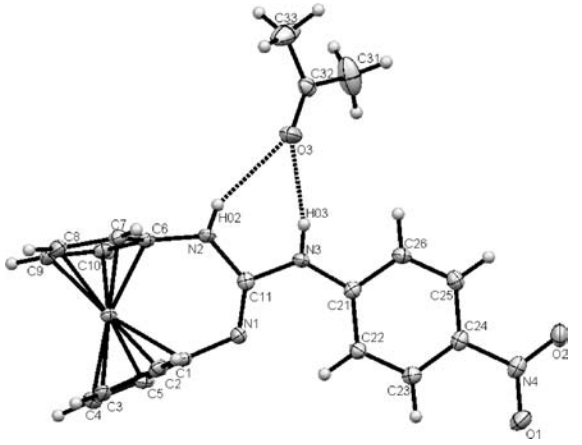

Figure 1. ORTEP view of the molecular structure of compound **4** showing the hydrogen bonds formed with the molecule of acetone. Thermal ellipsoids are drawn at 50% probability level.

perfectly planar but deviate from being parallel, that is, the angle between the planes is 15.7° and the rings are completely eclipsed. The organic ligand attached to the ferrocenyl moiety is almost planar, the deviation from the main plane including the nitro group being 0.0633 Å. The planarity is induced by the presence of acetone retained in the lattice.[23] The oxygen atom of the acetone forms two intermolecular N−H···O hydrogen bonds with the hydrogens of the amino groups of the organic moiety in a way that fix its conformation preventing the free rotation of N3−C21 bond. The C24−N4 bond is also hindered from rotation by the presence of some hydrogen bonds involving the oxygen atoms O1 and O2. The organic ligand adopts a nearly perpendicular orientation with respect to the Cp rings, the angle between mean planes being 85.9° (C1-ring) and 85.8° (C6-ring).

Regarding the crystal structure of **4**, molecules are interlinked by N2−H02···O1 and C7−H7···O2 hydrogen bonds (Table 1), forming layers perpendicular to the *c* axis (see crystal packing diagram of **4** in Supporting Information).

Compound **4** could exist in three tautomeric forms: ***4anti***, ***4syn***, and ***4imino*** (Chart 1). Thus, an in depth study about the tautomerism of both the neutral and the charged forms of **4** have been carried out through the comparison of the calculated and experimental chemical shifts obtained by ^{1}H, ^{13}C, and ^{15}N NMR

Table 1. Hydrogen Bonds [Å and deg][a]

D−H···A	*d*(D−H)	*d*(H···A)	*d*(D···A)	∠(DHA)
N(2)−H(02)···O(3)#1	0.82(3)	2.33(3)	3.033(2)	144(2)
N(3)−H(03)···O(3)#1	0.82(3)	2.09(3)	2.892(2)	165(2)
N(2)−H(02)···O(1)#2	0.82(3)	2.58(3)	3.181(2)	131(2)
C(7)−H(7)···O(2)#3	0.95	2.51	3.361(3)	149.8

[a] Symmetry transformations used to generate equivalent atoms: #1 $-x+1/2, -y, z+1/2$ #2 $-x+1/2, y-1/2, z$ #3 $x+1, y, z$.

Chart 1. Acid-Base Equilibria and Tautomeric Forms of Receptor 4 and 4^-

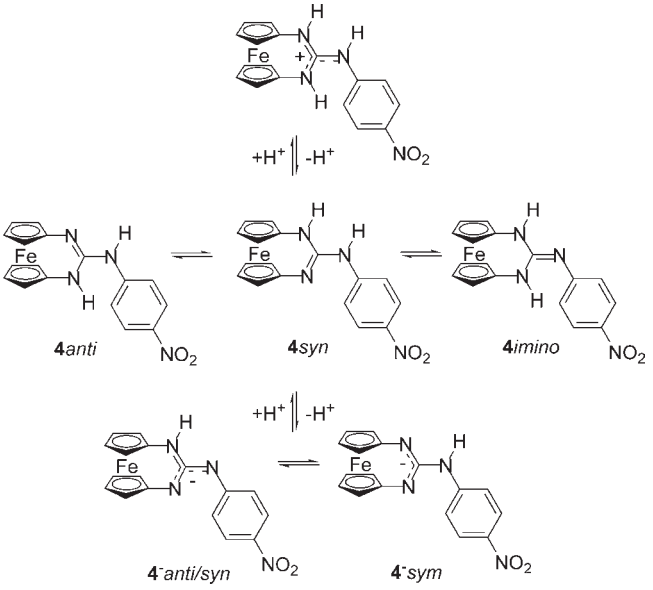

Table 2. Energies at the B3LYP/6-311++G(d,p) Level[a] **of Neutral, Anionic, and Cationic Forms**

structure	SCF energy	E_{rel}
4anti	−2289.58519	2.9
4syn	−2289.58564	1.7
4imino$^-$	−2289.58630	0.0
4^-***anti/syn***	−2289.05566	0.0
4^-***sym***	−2289.05230	8.8
$4\cdot H^+$	−2289.97252	

[a] Absolute values, hartree; relative values, kJ mol^{-1}.

experiments using different deuterated solvents, as well as through the calculated energies for these forms at the B3LYP/6-311++G-(d,p) level (Supporting Information). These results demonstrate that, in $CDCl_3$ solution, **4** is as a mixture in equilibrium of *syn* and *imino* forms in similar abundance (the two most stable according to the theoretical calculations reported in Table 2. In acetone-d_6, receptor **4** exists exclusively in the *syn* form, independently of the temperature, because of the formation of a bifurcated hydrogen bond with the solvent. Similarly, in the solid state (CPMAS NMR measurements, see Supporting Information), **4** also exists in the *syn* form because of the presence of acetone in the crystals. Analogous NMR studies carried out on the 4^- species demonstrate that this guanidinate anion exists exclusively in the *anti/syn* form (Supporting Information).

dx.doi.org/10.1021/ic102314r |*Inorg. Chem.* 2011, 50, 4212–4220

Chart 2. Tautomeric Forms of 4 and Related Structures for the NICS Calculations

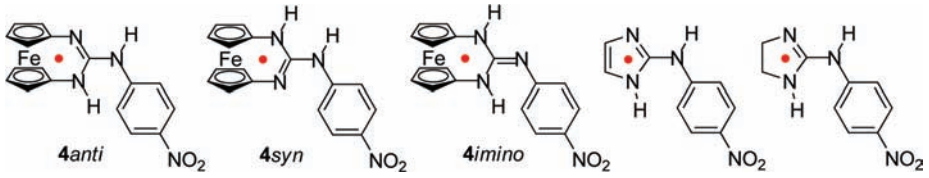

Table 3. Isotropic NICS Values (ppm)

structure	NICS(0)	NICS(+1)	NICS(−1)
4*anti*	1.8	1.8	0.3
4*syn*	2.0	1.5	1.2
4*imino*$^-$	2.5	0.9	0.8
imidazole	11.6	8.7	8.6
imidazoline	4.2	1.8	1.9

The nucleus-independent chemical shift (NICS) is a computational method that calculates the chemical shifts of a hypothetical lithium ion positioned directly inside the ring or, more recently, 1 Å above (+1) or below (−1) the ring.[24] In the original Schleyer definition negative NICS values indicate aromaticity and positive values antiaromaticity, but in the Gaussian implementation, the signs are reversed. Then, by using the Gaussian convention[25] nucleus-independent chemical shift calculations have been carried out for the three tautomers of **4**, yielding values between 0 and 2 ppm [both NICS(0) and NICS(1)] proving that the "ferrimidazole" ring is not aromatic and resembles more imidazolines [NICS(1) = 1.8 ppm] than imidazoles [NICS(1) = 8.7 ppm] (Chart 2 and Table 3).

Anion Recognition Studies. The recognition properties of receptor **4**, having a particularly effective neutral hydrogen bonding motif, toward various anions which possess spherical (F^-, Cl^-, Br^-), trigonal planar (AcO^-, $PhCO_2^-$, NO_3^-) or tetrahedral (HSO_4^-, $H_2PO_4^-$, $HP_2O_7^{3-}$) geometries have been investigated by electrochemistry, UV−vis spectroscopic measurements, and ^{1}H NMR spectroscopy.

As it was expected, receptor **4** shows electroactivity because of the Fe(II)/Fe(III) redox couple. In fact, CV of an electrochemical solution of **4**, ($c = 10^{-3}$ M in MeCN), containing 0.1 M TBAHP as supporting electrolyte gave rise to a quasi reversible oxidation wave at Ep = 440 mV versus decamethylferrocene (DCMF) when the oxidation was carried out in the range from 0 to 800 mV (Figure 2a). Working under the same electrochemical conditions but from 0 to 1100 mV, receptor **4** displays an additional nonreversible oxidation peak at ^2Ep = 817 mV versus DCMF which could be assigned to the oxidation of the C═N group present in the phane bridge, as has previously reported for related moieties such as formamidine[26] or 2-aza-1,3-butadiene bridges[27] Likewise, the DPV also exhibits two oxidation peaks at the same potentials (Figure 2b).

The electrochemical behavior of receptor **4** acidic media was also studied by addition of acetic acid to the electrochemical solution. While addition of acetic acid did not cause any effect on the OSWV of this species, giving rise to the two characteristic oxidation peaks at ^1Ep = 440 mV and ^2Ep = 817 mV. By contrast, addition of a stronger acid such as HBF_4 promotes the appearance of only one oxidation peak at Ep = 860 mV assigned to the monooxidation of the ferrocene unit within the guanidinium species [**4**·**H**$^+$] formed (Supporting Information)

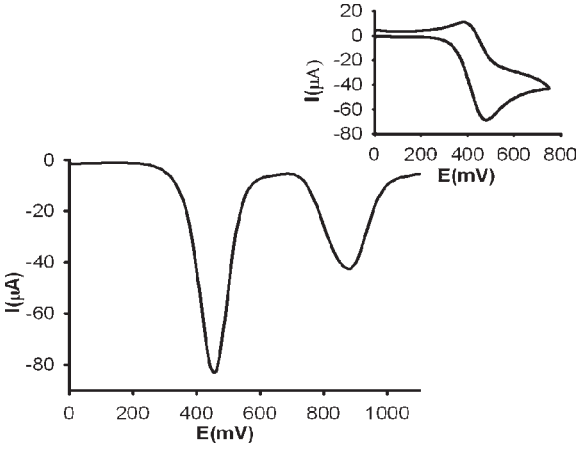

Figure 2. DPV, from 0.0 to 1.1 V of compound **4** (1 mM) in CH_3CN using $[(n\text{-}C_4H_9)_4N]PF_6$ (0.1 M) as supporting electrolyte. Inset: CV corresponding to receptor **4**, from 0.0 to 0.8 V.

The recognition capability of the receptor **4** toward the abovementioned set of anions, in the form of their corresponding tetrabutylammonium salts, was evaluated by DPV.[28] In general, the results obtained demonstrate that while addition of AcO^-, $PhCO_2^-$, NO_3^-, F^-, Cl^-, and Br^- anions promotes remarkable responses, addition of HSO_4^-, $H_2PO_4^-$, and $HP_2O_7^{3-}$ anionic species had no effect on the CV or DPV of this receptor, even when present in a large excess. Nevertheless, the results obtained on the stepwise addition of substoichiometric amounts of AcO^-, $PhCO_2^-$, NO_3^-, F^-, Cl^-, or Br^- anions revealed two different electrochemical behaviors. Thus, addition of increasing amounts of the basic AcO^-, $PhCO_2^-$, and F^- anions to the free ligand promotes the complete disappearance of the oxidation peak at Ep = 817 mV. Moreover, a typical "two wave behavior" was observed for the evolution of the peak at Ep = 440 mV, which consists in the progressive appearance of a second oxidation peak at more negative potentials (ΔEp = −182 mV for AcO^-, ΔEp = −152 mV for $PhCO_2^-$, and ΔEp = −128 mV for F^-) together with the corresponding to the free receptor, which completely disappeared when addition of 1 equiv of anion was achieved (Figure 3a and Supporting Information). This kind of electrochemical behavior has also been observed in biferrocene systems bearing guanidine bridges as anion binding sites.[10b,c] However, after addition of NO_3^-, Cl^-, and Br^- anions the two oxidation peaks are still observed, although negatively shifted compared to the free receptor ("shifting behavior").[29] Nevertheless, while the first oxidation peak was slightly cathodically shifted the second one was cathodically shifted in a larger values[30] (Figure 3b and Supporting Information). The difference between the potentials of the two peaks observed ($\Delta Ep = {}^2Ep - {}^1Ep$ = 377 mV), is decreased when the complexes between the receptor and the less basic NO_3^-, Cl^-, and Br^- anions are

dx.doi.org/10.1021/ic102314r |*Inorg. Chem.* 2011, 50, 4212–4220

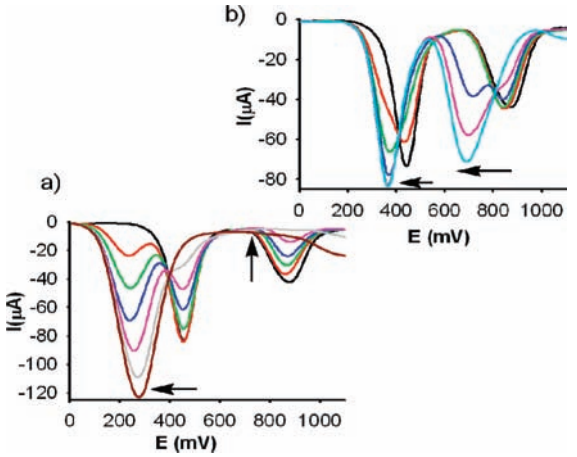

Figure 3. Evolution of the DPV of **4** (1 mM in CH_3CN), scanned at 0.1 V s^{-1} with $[(n\text{-}Bu)_4N]ClO_4$ as supporting electrolyte, upon addition of 0 to 3 equiv of: (a) AcO^- anion and (b) Cl^- anion.

formed: ΔEp = 265 mV for Cl^-, ΔEp = 242 mV for Br^-, and ΔEp = 258 mV for NO_3^-.

To get insight into the roles that the anions play when they are added to the free receptor **4**, two different titration experiments were carried out. On the one hand, upon titration with a strong base, such as Bu_4NOH, which can only promote the deprotonation of the free ligand, disappearance of the second oxidation peak and a considerable cathodic shift of the first oxidation peak were observed. (ΔEp = −228) (Supporting Information). On the other hand, titration experiments in the presence of AcOH (20 equiv) were also carried out to avoid any deprotonation effect. The results derived from these experiments, show that addition of AcO^-, $PhCO_2^-$, and F^- still gave rise to significant oxidation potential shifts although in a slightly smaller magnitude than those obtained from the free ligand, (ΔEp = −116 mV for AcO^-, ΔEp = −105 mV for $PhCO_2^-$ and ΔEp = −62 mV for F^-) anions (Supporting Information). The results obtained upon addition of AcO^-, $PhCO_2^-$, and F^- anions seems to suggest that in the absence of an acidic medium a recognition process should take place, the differences in the values of the oxidation waves being attributable to the changes promoted in the electrochemical solutions by the presence of the AcOH. Deprotonation processes should be ruled out because of the absence of any wave which could be attributable to the deprotonated species which should appear at higher oxidation potential values than those observed upon addition of these anions, even when they are added in a large excess.

Interestingly, addition of AcO^- anion to an electrochemical solution containing triethylamine induces a shift in the first oxidation peak of ΔEp = −70 mV, indicating that the recognition process is still taking place even under these conditions. By contrast, Cl^-, Br^-, and NO_3^- anions do not apparently promote any perturbation, which is indicative that the interaction between receptor **4** and these anions mainly involve hydrogen-bonded complex formation (Supporting Information).

Previous studies on ferrocene-based ligands have shown that their characteristic low energy (LE) bands in the absorption spectra are perturbed upon complexation.[31] Moreover, the chromogenic *p*-nitrophenyl group also provides a further advantage, allowing one to monitor complex formation through definite color changes and spectral modifications. Therefore, the occurrence of the receptor-anion interaction was also studied by the distinctive changes of the receptor's absorbance in the UV−vis

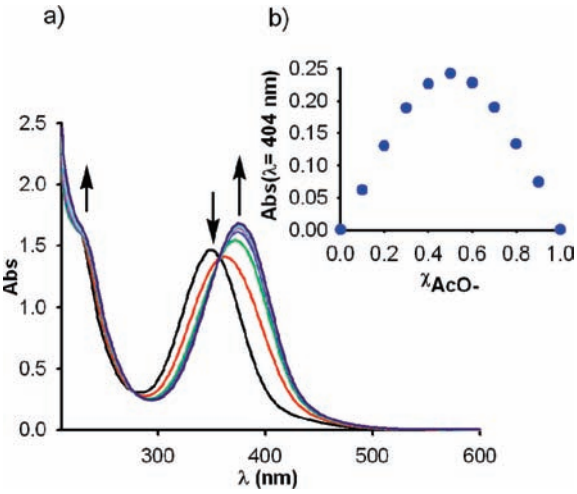

Figure 4. (a) Variation of the UV/vis in CH_3CN of ligand **4** ($c = 10^{-4}$ M) upon addition of increasing amounts of AcO^- anions, from 0 to 3 equiv. Arrows indicate the absorptions that increase (up) and decrease (down) during the experiments. (b): Job's plot evaluated from the absorption spectra of the titration solution exhibiting the inflection point at 0.5 (formation of a 1:1 complex): the total $[\mathbf{4}]^+$ $[AcO^-] = 10^{-4}$ M.

region. The UV−vis spectrum of receptor **4** in CH_3CN ($c = 1 \times 10^{-4}$ M) exhibits strong absorption bands at λ = 226 nm (ε = 16550 M^{-1} cm^{-1}) and 350 (ε = 14710 M^{-1} cm^{-1}) nm. Figure 4 shows the family of spectra taken in the course of the titration receptor **4**, with the Y-shaped anion AcO^-, in a MeCN solution. Upon addition of AcO^-, the band at 350 nm (ε = 14710 M^{-1} cm^{-1}) progressively decreases, while a new band at 374 nm (ε = 16770 M^{-1} cm^{-1}) ($\Delta\lambda$ = 24 nm) is formed and developed (Table 3). The presence of two sharp isosbestic points at 276 and 357 nm indicates that only two species coexist in the equilibrium.

Analogous investigations were also carried out by using $PhCO_2^-$, F^-, Cl^-, Br^-, NO_3^-, HSO_4^-, $H_2PO_4^-$, and $HP_2O_7^{3-}$. For $PhCO_2^-$ and F^- anions, spectral features are the same as those observed for AcO^- anion, whereas no spectral changes were observed for NO_3^-, HSO_4^-, $H_2PO_4^-$, and $HP_2O_7^{3-}$ anions, and a small red-shift ($\Delta\lambda$ = 6 nm) of the absorption band was observed for Br^-, Cl^- anions (Supporting Information). Addition of Bu_4NOH, however, induced the appearance of an additional low-energy band at 481 nm ($\Delta\lambda$ = 11 nm) attributable to the deprotonated species, which is responsible for the development of a deep orange-red color in the solution. Thus, deprotonation seems to be signaled by the appearance of a new absorption band at a longer wavelength, taking only place in the case of adding hydroxide anion (Supporting Information).

For AcO^-, and $PhCO_2^-$ anions, binding assays using titration isotherms suggest a 1:1 binding model. The corresponding association constants were determined by treatment of the spectrophotometric titration data,[32] the values obtained being those shown in Table 4. Moreover, the calculated detection limits[33] were 1.0×10^{-5} M for both AcO^- and $PhCO_2^-$ anions, 2.8×10^{-5} M for F^-, 2.2×10^{-5} M for Cl^-, and 3.4×10^{-5} M for Br^-.

For the reported constants to be taken with confidence, we have proved the reversibility of the complexation processes. If the sensing system is reversible, depletion of the anion that coordinates **4** must produce a change of the absorption spectrum, causing it to revert to the original spectrum. Formation of the complexes $\mathbf{4}\cdot AcO^-$ or $\mathbf{4}\cdot PhCO_2^-$ and the subsequent decomplexation by extraction of the anion with H_2O were carried out

dx.doi.org/10.1021/ic102314r |*Inorg. Chem.* 2011, 50, 4212–4220

Table 4. Relevant Data of the Ligand/Anion Complexes Formed

	$\Delta\lambda^a$	$K_{as}{}^b$	$\Delta H_A{}^c$	$\Delta H_B{}^d$
$4\cdot AcO^-$	24	3.54×10^3 ($\pm$0.39)	+0.27	−0.09
$4\cdot PhCO_2^-$	24	3.64×10^3($\pm$0.36)	+0.37	−0.05
$4\cdot F^-$		7.3×10^4 ($\pm$1.20)	+0.16	−0.05
$4\cdot Cl^-$	6	4.8×10^4 ($\pm$1.28)	+0.17	−0.06
$4\cdot Br^-$	6	6.3×10^3 ($\pm$1.56)	+0.19	−0.05
$[4\cdot H^+]$	−58		−0.18	+0.24
$[4\cdot H^+]\cdot Cl^-$ [e]	8	4.0×10^5 ($\pm$0.18)	−0.13	−0.09
$[4\cdot H^+]\cdot Br^-$ [e]	8	2.8×10^4 ($\pm$0.11)	−0.05	−0.02
$[4\cdot H^+]\cdot NO_3^-$ [e]	8	1.6×10^4 ($\pm$0.07)	−0.11	−0.03

[a] Shift, in nm, of the LE band upon complexation $\Delta\lambda = \lambda_{(complexed)} - \lambda_{(free\ ligand)}$. [b] Association constant, in M^{-1}, determined, from the UV−vis titration data, by Specfict/32 Global Analysis System. [c] $\Delta H_A = H_{A(complexed)} - H_{A(free\ ligand)}$, in ppm. [d] $\Delta H_B = H_{B(complexed)} - H_{B(free\ ligand)}$ in ppm. [e] For the calculation of these data, the values of the variables corresponding to the $[4\cdot H^+]$ species were taken as reference.

over several cycles. The optical spectra were recorded after each step and found to be fully recovered on completion of the step, thus demonstrating the high degree of reversibility of the sensing process (Supporting Information).

With the view to shedding some light on the structure of complex formation of this receptor **4**, we carried out ^{1}H NMR titration experiments upon addition of increasing amounts of a solution of the aforementioned anions to an acetone-d_6 solution of **4**. CD_3CN was chosen as a solvent of the anions to afford a concentration suitable for ^{1}H NMR spectroscopic studies ($c = 2.5 \times 10^{-2}$ M). The free receptor shows two characteristic broad singlets, at δ = 3.94 ppm and δ = 4.09 ppm, integrating 4H each, corresponding to the H_α+$H_{\alpha'}$ and H_β+$H_{\beta'}$ protons, respectively, within the two monosubstituted cyclopentadienyl (Cp) units present in the ferrocene moiety. Additionally, in the aromatic region, it exhibits the typical AB pattern of signals corresponding to the H_A and H_B protons present in the nitrophenyl substituent. It is worth mentioning that in the free ligand the signals corresponding to the guanidine protons do not appear when the spectrum was carried out at room temperature, probably because the tautomeric equilibrium is fast on the NMR time scale. However, when the ^{1}H NMR spectrum was obtained at −55 °C two significant features were observed: (i) the appearance of two broad singlets in the ferrocene region at δ = 4.11 ppm and δ = 3.85 ppm, integrating 6H and 2H, respectively; and (ii) the presence of two additional broad singlets at δ = 7.03 ppm and δ = 9.11 ppm, attributable to the guanidine NH protons.

^{1}H NMR titrations of **4** with the above-mentioned set of anions clearly evidenced that only the addition of AcO^-, $PhCO_2^-$, F^-, Cl^-, and Br^- promoted significant perturbations on the proton signals of this receptor. Two common features, in the regions of the ferrocene and aromatic protons, were observed during the titration experiments. These features are illustrated in Figure 5 corresponding to the spectra taken over the course of the titration with AcO^-. On the one hand, it illustrates the spectral shifts of the H_A and H_B, aromatic protons present in the phenyl ring linked to the guanidine moiety indicating the formation of a discrete H-bond complex. In fact, two effects are expected to derive from the hydrogen bond formation between the guanidine subunit and the anion: (i) the increase of electron density in the phenyl rings, with a through-bond propagation; this fact causes a shielding effect and should

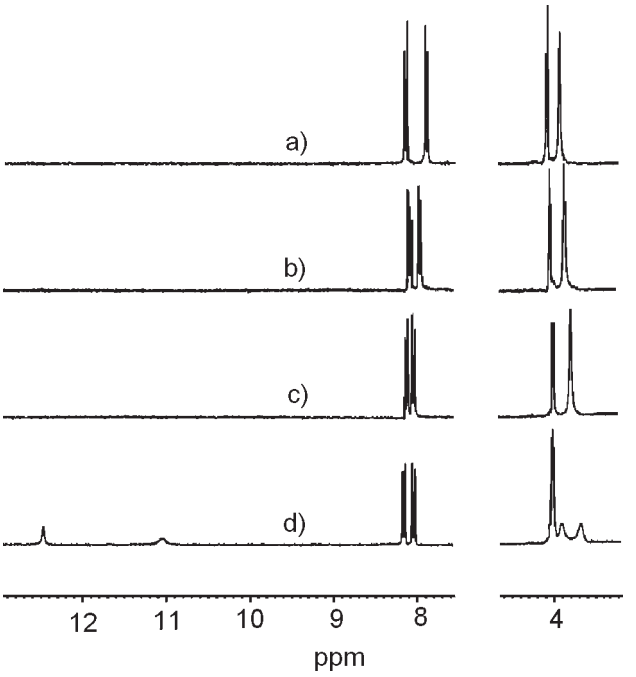

Figure 5. Evolution of the ^{1}H NMR spectra of **4** in acetone-d_6 upon addition of AcO^-, from (a) 0 to (d) 1 equiv.

promote an upfield shift; (ii) the polarization of the C−H bonds, induced by a through-space effect, in particular the partial positive charge created onto the proton, causes a deshielding effect and promotes a downfield shift. The latter effect is expected to vanish at higher distances and should therefore operate only on the $C-H_A$ bond. In fact, in the case of the $C-H_A$ proton, the electrostatic effect dominates, and a progressive downfield shift ($\Delta\delta$ = 0.27 ppm) is observed. On the other hand, $C-H_B$ protons feel neither the anion-induced electrostatic effect nor the $C-H_A$ polarization effect, thus being affected only by the through-bond effect, which induces a moderate upfield shift ($\Delta\delta$ = −0.09 ppm)[34] (Table 4). On the other hand, some interesting facts are also detected in the ferrocene region: while the broad singlet corresponding to the H_β and $H_{\beta'}$ protons remained almost unaltered the one corresponding to the H_α and $H_{\alpha'}$ is now split into two new broad singlets, one appearing at a chemical shift (δ = 3.91 ppm), almost equivalent to that observed in the free ligand (δ = 3.94 ppm), and another one (δ = 3.69 ppm) upfield shifted by $\Delta\delta$ = 0.10 ppm. Moreover, addition of AcO^- promotes the appearance of two new singlets at δ = 11.05 ppm and δ = 12.47 ppm which could be associated to the guanidine NH protons. The last observations are in agreement with the results obtained when the ^{1}H NMR spectrum of the free ligand **4** was carried out at −55 °C.

This anion-induced chemical shift changes in the ^{1}H NMR spectra of **4**, suggesting that both NH guanidine protons are involved in the complexation of this anion which prevent, to some extent, both the tautomeric effect and the free rotation of the aryl group linked to the C2 of the ferrocenophane framework thus making the Cp rings of the ferrocene units non-equivalent and, as a consequence, justifying the appearance of two different signals for the H_α and $H_{\alpha'}$ protons of the ferrocene unit (Chart 3).

Completely analogous results were also obtained when the $PhCO_2^-$ anion was used as analyte (Table 4 and Supporting Information), also indicating that this anion is interacting with

dx.doi.org/10.1021/ic102314r |*Inorg. Chem.* 2011, 50, 4212–4220

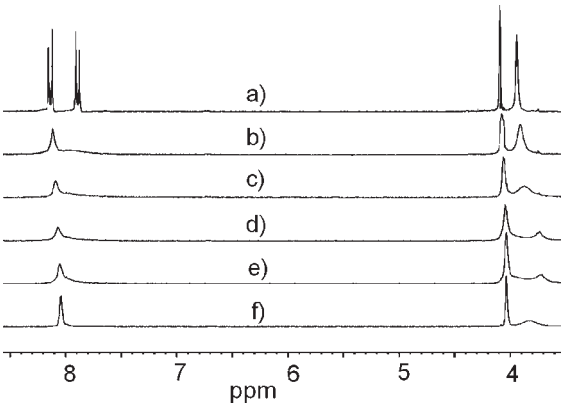

Figure 6. Evolution of the ^{1}H NMR spectra of **4** in acetone-d_6 upon addition of F^-, from (a) 0 to (f) 1 equiv.

Chart 3. Plausible Binding Mode in the Complex $[4\cdot AcO^-]$

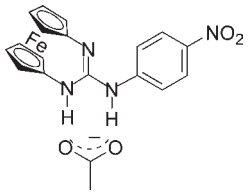

the free receptor via possible bonding between the anion and the guanidine moiety.

^{1}H NMR titration experiments with F^- (H_B $\Delta\delta = -0.05$; H_A $\Delta\delta = 0.16$ ppm), Cl^- (H_B $\Delta\delta = -0.06$; H_A $\Delta\delta = 0.17$ ppm), Br^- (H_B $\Delta\delta = -0.05$; H_A $\Delta\delta = 0.19$ ppm) showed also similar patterns than those observed with AcO^- anion (Table 4), although in these cases the two signals due to the aromatic protons are almost overlapped and no signals corresponding to the guanidine protons were observed. Moreover, the Hα protons within the ferrocene moiety appeared as a very broad singlet with very low intensity (Figure 6).

Because it is very well-known that the guanidinium group is an extremely effective functional unit in the binding of anionic species we decided to transform the guanidine moiety within the receptor **4** into the corresponding guanidinium specie $[4\cdot H]^+$, by treatment with 1 equiv of HBF_4 in MeCN.

The electrochemical response of **4** after addition of HBF_4 was previously studied by using CV and DPV and a 0.1 M solution of TBAHP as supporting electrolyte (Supporting Information). As expected, the protonation process resulted in the appearance, at E_p = 860 mV, of a new oxidation peak anodically shifted (ΔEp = 420 mV) with reference to the free receptor.

The $[4\cdot H]^+$ guanidinium receptor has also been used to investigate its ability for sensing the anion binding by using the previously mentioned set of anions: F^-, Cl^-, Br^-, AcO^-, $PhCO_2^-$, NO_3^-, HSO_4^-, $H_2PO_4^-$, and $HP_2O_7^{3-}$. While the tetrahedral oxoanions used do not promote any changes in the oxidation potential of the ferrocene unit, addition of AcO^-, $PhCO_2^-$, and F^- anions induced the appearance of a new oxidation peak, which is cathodically shifted. The evolving peak, appeared at virtually the same potential than that of the free receptor **4**, indicating that a deprotonation has taken place (Figure 7a). However, the addition of Cl^-, Br^-, and NO_3^- anions elicited a different electrochemical response (Figure 7b

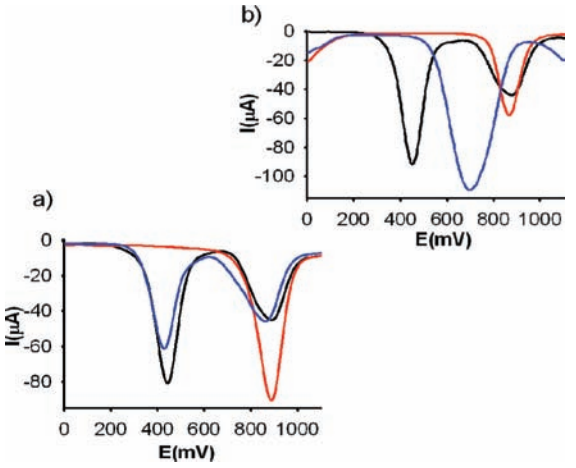

Figure 7. Evolution of the DPV of $4\cdot H^+$ (1 mM in CH_3CN), (red line) scanned at 0.1 V s^{-1} with $[(n\text{-}Bu)_4N]ClO_4$ as supporting electrolyte, upon addition of (a) 1 equiv of AcO^- (blue line) and (b) 3 equiv of Cl^- anion (blue line). Black lines in (a) and (b) correspond to the DPV of the free ligand **4**.

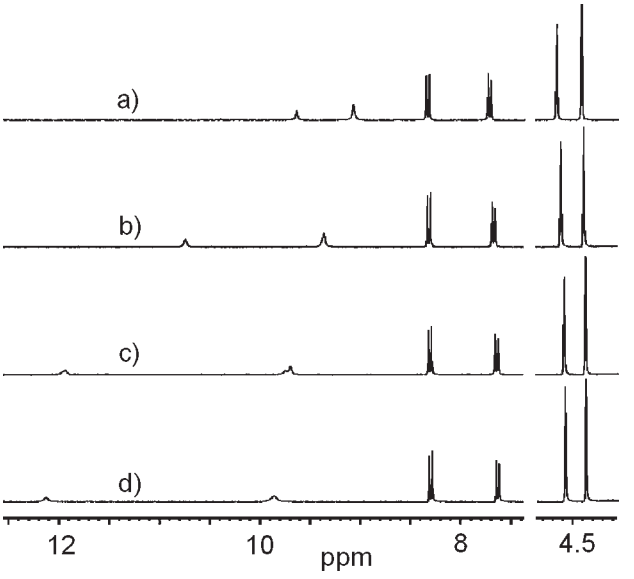

Figure 8. Evolution of the ^{1}H NMR spectra of $[4\cdot H^+]$ in acetone-d_6 upon addition of Cl^- anion, from (a) 0 to (d) 1 equiv.

and Supporting Information). In such cases the redox peak is cathodically shifted: $\Delta Ep = -170$ mV for Cl^- and NO_3^- anions and $\Delta Ep = -200$ mV for Br^-.

The ^{1}H NMR spectrum of the receptor **4** is also strongly perturbed upon protonation with HBF_4 in deuterated MeCN. Then, the ^{1}H NMR spectrum of the resulting complex $[4\cdot H^+]$ displays two singlets at 11.40 and 9.61 ppm due to the N−H protons. The aromatic H_B protons are downfield shifted by 1.8 ppm and the H_A protons are upfield shifted in almost the same extension. Moreover, both pseudotriplets due to the protons within the cyclopentadienyl rings are downfield shifted by 0.56 and 0.46 ppm, respectively. Addition of 1 equiv of AcO^-, $PhCO_2^-$, and F^- anions to a solution of $[4\cdot H^+]$ induces a deprotonation effect and, as a consequence, the spectrum of the free receptor **4** is recovered (Supporting Information). However, in the presence of Cl^- (Figure 8) ($\Delta\delta = 0.97$ ppm), Br^- ($\Delta\delta = 0.44$ ppm),

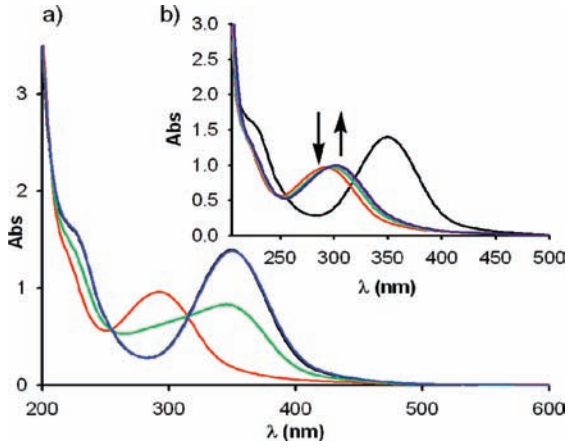

Figure 9. Variation of the UV/vis in CH_3CN of ligand $\mathbf{4}\cdot\mathbf{H}^+$ ($c = 10^{-4}$ M) upon addition of (a) 1 equiv of AcO^- and (b) 1 equiv of Br^- anions. Arrows indicate the absorptions that increase (up) and decrease (down) during the experiments.

and NO_3^- ($\Delta\delta$ = 0.61 ppm) anions, the signals corresponding to the N−H protons are remarkably downfield shifted, while the remaining signals are not apparently perturbed (Supporting Information).

Salient features of UV−vis spectrum of the complex $[\mathbf{4}\cdot H^+]$ when compared to that of the free receptor is the appearance of a low-energy band at 292 nm, which is blue-shifted by $\Delta\lambda$ = 52 nm. However, upon addition of 1 equiv of AcO^-, $PhCO_2^-$, and F^- anions the original absorption spectrum of the free receptor **4** is recovered (Figure 9a). By contrast, in the presence of Cl^-, Br^-, and NO_3^- anions the low-energy band is red-shifted by $\Delta\lambda$ = 8 nm (Figure 9b). In this case, the presence of two isosbestic points around 252 and 292 nm indicates that only two species coexist at the equilibrium.

The binding isotherms were fitted to a 1:1 binding stoichiometry, and the binding constants were found to be $K_a = 4.0 \times 10^5$ (±0.18) M^{-1} for Cl^-, $K_a = 2.8 \times 10^4$ (±0.11) M^{-1} for Br^-, and $K_a = 1.6 \times 10^4$ (±0.07) M^{-1} for NO_3^- anion. As it was expected, these values are higher than those found for the free receptor toward the same anions. The 1:1 stoichiometry of the complexes formed between the guanidinium receptor $[\mathbf{4}\cdot H^+]$ and these anions was also confirmed by electrospray ionization mass spectrometry, in which the peaks [$\mathbf{4}\cdot H^+$-anion] were observed (Supporting Information). Additionally, the calculated detection limits were 10^{-5} M for Cl^-, 2.0×10^{-5} M for Br^-, and 2.8×10^{-5} M for NO_3^- anions.

In summary, the electrochemical, ^1H NMR and UV−vis data underscore the binding ability of the guanidinium receptor $[\mathbf{4}\cdot H^+]$ for the less basic Cl^-, Br^-, and NO_3^- anions in MeCN.

CONCLUSION

We have designed a new guanidinoferrocene-based receptor **4** which exists in the *syn* form in the solid state. In $CDCl_3$ solution appears as a mixture of *syn* and *imino* forms in similar abundance, whereas in acetone exclusively exists in the *syn* form.

Because of the amphoteric nature of the guanidine unit, it displays an interesting pH-dependent redox behavior, ranging the Fe(II)/Fe(III) redox couple from *Ep* = 212 mV for the deprotonated form to *Ep* = 860 mV for the monoprotonated form (ΔEp = 648 mV). It allows the sensing of AcO^-, $PhCO_2^-$, F^-, Cl^-, and Br^- anions through an unusual redox ratiometric fashion and spectroscopic (^1H NMR and UV−vis) measurements. Its monoprotonated form $[\mathbf{4}\cdot\mathbf{H}^+]$ is able to selectively sense the less basic Cl^-, Br^-, and NO_3^- anions: the oxidation redox peak is cathodically shifted (170−200 mV), and the low-energy band of the absorption spectrum is red-shifted ($\Delta\lambda$ = 8 nm) upon complexation. In addition, the signals due to the NH protons in the ^1H NMR spectrum are remarkably downfield shifted (0.44−0.97 ppm).

ASSOCIATED CONTENT

Supporting Information. Electrochemical. ^1H and ^{13}C NMR of **4**. Electrochemical and spectroscopic titration data. CPMAS spectra. Theoretical calculations. X-ray data. This material is available free of charge via the Internet at http://pubs.acs.org.

AUTHOR INFORMATION

Corresponding Author

*E-mail: pmolina@um.es; (P.M.), atarraga@um.es (A.T.).

ACKNOWLEDGMENT

We gratefully acknowledge the financial support from MICINN-Spain, Project CTQ2008-01402, CTQ2009-13129-C02-02, CTQ2010-16122 and Fundación Séneca (Agencia de Ciencia y Tecnología de la Región de Murcia) project 04509/GERM/06 (Programa de Ayudas a Grupos de Excelencia de la Región de Murcia, Plan Regional de Ciencia y Tecnología 2007/2010) and the Comunidad Autónoma de Madrid (Project MADRISOLAR2, ref S2009/PPQ-1533). We deeply acknowledge the CTI (CSIC) for an allocation of computer time.

DEDICATION

†A tribute in memory of the Organic Chemistry Professor Dr. Rafael Suau Suarez (University of Málaga, Spain).

REFERENCES

(1) Sessler, J. L.; Gale, P. A.; Cho, W. S. *Anion Receptor Chemistry*; The Royal Society of Chemistry: Cambridge, 2006.

(2) (a) Caltagirone, C.; Gale, P. A. *Chem. Soc. Rev.* **2009**, *38*, 520–563. (b) Gale, P. A.; García-Garrido, S. E.; Garric, J. *Chem. Soc. Rev.* **2008**, *37*, 151–190.

(3) Hannon, C. L.; Anslyn, E. V. In *Biorganic Chemistry Frontiers*; Duggas, H.; Schidtchen, F. P., Eds.; Springer: Berlin, 1993; Vol. 3, pp 193−255.

(4) (a) Best, M. D.; Tobey, S. L.; Anslyn, E. V. *Coord. Chem. Rev.* **2003**, *240*, 3–15. (b) Müller, G.; Riede, J.; Schmidtchen, F. P. *Angew. Chem., Int. Ed. Engl.* **1988**, *27*, 1516–1518. (c) Schug, K. A.; Lindner, W. *Chem. Rev.* **2005**, *105*, 67–113. (d) Seel, C.; Galan, A.; de Mendoza, J. *Top. Curr. Chem.* **1995**, *175*, 101–132. (e) Berger, M.; Schmidtchen, F. P. *Chem. Rev.* **1997**, *97*, 1609–1646. (f) Orner, B. P.; Hamilton, A. D. *J. Inclusion Phenom. Macrocyclic Chem.* **2001**, *41*, 141–147. (g) Houk, R. J. T.; Tobey, S. L.; Anslyn, E. V. *Top. Curr. Chem.* **2005**, *255*, 199–229. (h) Blondeau, P.; Segura, M.; Pérez-Fernández, R.; de Mendoza, J. *Chem. Soc. Rev.* **2007**, *36*, 198–210. (i) Jadhav, V. D.; Herdtweck, E.; Schmidchen, F. P. *Chem.—Eur. J.* **2008**, *14*, 6098–6107.

(5) (a) Baily, P. J.; Pace, S. *Coord. Chem. Rev.* **2001**, *214*, 91–141. (b) Coles, M. P. *Chem. Commun.* **2009**, 3659–3676.

(6) (a) Coles, M. P. *Dalton. Trans.* **2006**, 985–1001. (b) Khalaf, M. S.; Oakley, S. H.; Coles, M. P.; Hitchcok, P. B. *Dalton Trans.* **2010**, *39*, 1635–1642.

(7) (a) Ratilla, E. M. A.; Kostic, N. M. *J. Am. Chem. Soc.* **1998**, *120*, 4427–4428. (b) Ratilla, E. M. A.; Scout, B. K.; Moxness, M. S.; Kostic, N. M. *Inorg. Chem.* **1990**, *29*, 918–926. (c) Aioki, S.; Iwaida, K.; Hanamoto, N.; Shiro, M.; Kimura, E. *J. Am. Chem. Soc.* **2002**, *124*, 5226–5257.

(8) (a) Beer, P. D. *Chem. Soc. Rev.* **1989**, *18*, 409–450. (b) Beer, P. D.; Gale, P. A.; Chen, G. Z. *Coord. Chem. Rev.* **1999**, *185*−*186*, 3–36. (c) Molina, P.; Tárraga, A.; Caballero, A. *Eur. J. Inorg. Chem.* **2008**, 3401–3417.

(9) (a) Otón, F.; Tárraga, A.; Velasco, M. D.; Espinosa, A.; Molina, P. *Chem. Commun.* **2004**, 1628–1659. (b) Otón, F.; Tárraga, A.; Velasco, M. D.; Espinosa, A.; Molina, P. *Dalton. Trans.* **2005**, 1159–1161. (c) Otón, F.; Tárraga, A.; Espinosa, A.; Velasco, M. D.; Bautista, D.; Molina, P. *J. Org. Chem.* **2005**, *70*, 6603–6608. (d) Otón, F.; Tárraga, A.; Espinosa, A.; Velasco, M. D.; Molina, P. *J. Org. Chem.* **2006**, *71*, 4590–4598. (e) Otón, F.; Tárraga, A.; Espinosa, A.; Velasco, M. D.; Molina, P. *Dalton Trans.* **2006**, 3685–3692. (f) Zapata, F.; Caballero, A.; Espinosa, A.; Tárraga, A.; Molina, P. *J. Org. Chem.* **2008**, *73*, 4034–4044. (g) Otón, F.; Espinosa, A.; Tárraga, A.; Ratera, I.; Wurst, K.; Veciana, J.; Molina, P. *Inorg. Chem.* **2009**, *48*, 1566–1576. (h) Romero, T.; Caballero, A.; Tárraga, A.; Molina, P. *Org. Lett.* **2009**, *11*, 3466–3469. (i) Zapata, F.; Caballero, A.; Tárraga, A.; Molina, P. *J. Org. Chem.* **2010**, *75*, 162–169.

(10) (a) Beer, P. D.; Drew, M. G. B.; Smith, D. K. *J. Organomet. Chem.* **1997**, *543*, 259–261. (b) Otón, F.; Tárraga, A.; Molina, P. *Org. Lett.* **2006**, *8*, 2107–2110. (c) Otón, F.; Espinosa, A.; Tárraga, A.; Ramirez de Arellano, C.; Molina, P. *Chem.—Eur. J.* **2007**, *13*, 5742–5752.

(11) (a) Becke, A. D. *Phys. Rev. A* **1988**, *38*, 3098–3100. (b) Becke, A. D. *J. Chem. Phys.* **1993**, *98*, 5648–5652. (c) Lee, C.; Yang, W.; Parr, R. G. *Phys. Rev. B* **1988**, *37*, 785–789. (d) Hariharan, P. A.; Pople, J. A. *Theor. Chim. Acta* **1973**, *28*, 213–222.

(12) McIver, J. W.; Komornicki, A. K. *J. Am. Chem. Soc.* **1972**, *94*, 2625–2633.

(13) (a) Ditchfield, R.; Hehre, W. J.; Pople, J. A. *J. Chem. Phys.* **1971**, *54*, 724–728. (b) Frisch, M. J.; Pople, J. A.; Binkley, J. S. *J. Chem. Phys.* **1984**, *80*, 3265–3269.

(14) (a) Schleyer, P. v. R.; Maerker, C.; Dransfeld, A.; Jiao, H.; Hommes, N. J. R. v. *J. Am. Chem. Soc.* **1996**, *118*, 6317–6318. (b) Schleyer, P. v. R.; Manoharan, M.; Wang, Z. X.; Kiran, B.; Jiao, H.; Puchta, R.; Eikema Hommes, N. J. R. v. *Org. Lett.* **2001**, *3*, 2465–2468. (c) Steinmann, S. N.; Jana, D. F.; Wu, J. I.-C.; Schleyer, P. v. R.; Mo, Y.; Corminboeuf, C. *Angew. Chem., Int. Ed.* **2009**, *48*, 9828–9833. (d) Wang, Y.; Wu, J. I.; Li, Q.; Schleyer, P. v. R. *Org. Lett.* **2010**, *12*, 4824–4827.

(15) (a) Ditchfield, R. *Mol. Phys.* **1974**, *27*, 789–807. (b) London, F. *J. Phys. Radium.* **1937**, *8*, 397–409.

(16) Frisch, M. J.; Trucks, G. W.; Schlegel, H. B. et al. *Gaussian 03*, revision B.05; Gaussian, Inc.: Pittsburgh, PA, 2003.

(17) (a) Bader, R. F. W. *Atoms in Molecules: A Quantum Theory; The International Series of Monographs of Chemistry*; Halpen, J., Green, M. L. H., Eds.; Clarendon Press: Oxford, 1990. (b) Popelier, P. L. A. *Atoms in Molecules: An Introduction*; Prentice Hall: New York, 2000.

(18) (a) Popelier, P. L. A. *Chem. Phys. Lett.* **1994**, *228*, 160–164. (b) Rafat, M.; Devereux, M.; Popelier, P. L. A. *J. Mol. Graphics Modell.* **2005**, *24*, 111–120.

(19) (a) Blanco, F.; Alkorta, I.; Elguero, J. *Magn. Reson. Chem.* **2007**, *45*, 797–800. (b) Silva, A. M. S.; Sousa, R. M. S.; Jimeno, M. L.; Blanco, F.; Alkorta, I.; Elguero, J. *Magn. Reson. Chem.* **2008**, *46*, 859–864.

(20) (a) Molina, P.; Vilaplana, M. J. *Synthesis* **1994**, 1197–1218. (b) Fresneda, P. M.; Molina, P. *Synlett* **2004**, 1–17. (c) Arques, A.; Molina, P. *Curr. Org. Chem.* **2004**, *8*, 827–843.

(21) Tárraga, A.; Otón, F.; Espinosa, A.; Velasco, M. D.; Molina, P.; Evans, D. J. *Chem. Commun.* **2004**, 458–459.

(22) (a) Molina, P.; Arques, A.; Alias, A.; Foces−Foces, M. C.; Llamas−Saiz, A. L. *J. Chem. Soc., Chem. Commun.* **1992**, 424–426. (b) Molina, P.; Arques, A.; Alias, A. *J. Org. Chem.* **1993**, *58*, 5264–5270.

(23) All attempts to obtain acetone-free crystals suitable for X-ray diffraction studies were unsuccessful.

(24) (a) Chen, Z.; Wannere, C.-S.; Corminboeuf, C.; Puchta, R.; Schleyer, P. v. R. *Chem. Rev.* **2005**, *105*, 3842–3888. (b) Schleyer, P. v. R.; Maerker, C.; Dransfeld, A.; Jiao, H.; Eikema Hommes, B. J. R. v. *J. Am. Chem. Soc.* **1996**, *118*, 6317–6318.

(25) Alkorta, I.; Blanco, F.; Elguero, J.; Claramunt, R. M. *Tetrahedron* **2010**, *66*, 2863–2868, and references therein.

(26) (a) Daoust, B.; Lessard, J. *Can. J. Chem.* **1995**, *73*, 362–374. (b) Barbey, G.; Caullet, C. *Tetrahedron Lett.* **1977**, *18*, 3937–3938.

(27) Lloveras, V.; Caballero, A.; Tárraga, A.; Velasco, M. D.; Espinosa, A.; Wurst, K.; Evans, D. J.; Vidal-Gancedo, J.; Rovira, C.; Molina, P.; Veciana, J. *Eur. J. Inorg. Chem.* **2005**, 2436–2450.

(28) The DPV technique has been employed to obtain well-resolved potential information, because the individual redox processes are poorly resolved in the CV experiments, the individual $E_{1/2}$ potentials cannot easily be extracted from this data accurately. See: Serr, B. R.; Andersen, K. A.; Elliot, C. M.; Anderson, O. P. *Inorg. Chem.* **1988**, *27*, 4499–4504.

(29) Miller, S. R.; Gustowski, D. A.; Chen, Z. H.; Gokel, G. W.; Echegoyen, L.; Kaifer, A. E. *Anal. Chem.* **1988**, *60*, 2021–2024.

(30) ^1Ep = 365 mV (Δ^1Ep = − 75 mV) and ^2Ep = 630 mV (Δ^2Ep = − 187 mV) for Cl^-; ^1Ep = 375 mV (Δ^1Ep = − 65 mV) and ^2Ep = 617 mV (Δ^2Ep = − 200 mV) for Br^-; and ^1Ep = 384 mV (Δ^1Ep = − 56 mV) and ^2Ep = 642 mV (Δ^2Ep = − 175 mV) for NO_3^-.

(31) (a) Marder, S. R.; Perry, J. W.; Tiemann, B. G. *Organometallics* **1991**, *10*, 1896–1901. (b) Coe, B. J.; Jones, C. J.; McCleverty, J. A.; Bloor, D.; Cross, G. J. *J. Organomet. Chem.* **1994**, *464*, 225–232. (c) Müller, T. J.; Netz, A.; Ansorge, M. *Organometallics* **1999**, *18*, 5066–5074. (d) Carr, J. D.; Coles, S. J.; Asan, M. B.; Hurthouse, M. B.; Malik, K. M. A.; Tucker, J. H. R. *J. Chem. Soc., Dalton Trans.* **1999**, 57–62.

(32) *Specfit/32 Global Analysis System*; Spectrum Software Associates: Singapore, 1999−2004; http:www.bio−logic.info/spectfitsup/index.html. The Specfit program was acquired from Bio−logic, S.A. in January 2005. The equation to be adjusted by nonlinear regression using the above mentioned software was $\Delta A/b = \{K_{11}\Delta\varepsilon_{HG}[H]_{tot}[G]\}/\{1 + K_{11}[H]\}$, where H = host, G = guest, HG = complex, ΔA = variation in the absorption, b = cell width, K_{11} = association constant for a 1:1 model, and $\Delta\varepsilon_{HG}$ = variation of molar absorptivity.

(33) Shortreed, M.; Kopelman, R.; Kuhn, M.; Hoyland, B. *Anal. Chem.* **1996**, *68*, 1414–1418.

(34) (a) Boiocchi, M.; Del Boca, L.; Gómez, D. E.; Fabbrizzi, L.; Licchelli, M.; Monzani, E. *J. Am. Chem. Soc.* **2004**, *126*, 16507–16514. (b) Boiocchi, M.; Del Boca, L.; Esteban-Gómez, D.; Fabbrizzi, L.; Licchelli, M.; Monzani, E. *Chem.—Eur. J.* **2005**, *11*, 3097–3104. (c) Amendola, V.; Bergamaschi, G.; Boiocchi, M.; Fabbrizzi, L.; Milani, M. *Chem.—Eur. J.* **2010**, *16*, 4368–4380.